Effects of intrinsic oscillations on weight dynamics under Spike timing-dependent plasticity

Fabiano Baroni, Pablo Varona

EFFECTS OF INTRINSIC OSCILLATIONS ON WEIGHT DYNAMICS UNDER SPIKE TIMING-DEPENDENT PLASTICITY

Fabiano Baroni
GNB, Escuela Politecnica Superior
Universidad Autonoma de Madrid, Spain
fabiano.baroni@uam.es

Pablo Varona
GNB, Escuela Politecnica Superior
Universidad Autonoma de Madrid, Spain
pablo.varona@uam.es

ABSTRACT
Spike timing-dependent plasticity (STDP) is a form of Hebbian learning which is thought to underlie structure formation during development, and learning and memory in later life. In this paper we show that the intrinsic properties of the postsynaptic neuron might have a deep influence on STDP dynamics, by shaping the causal correlation between the pre and the postsynaptic spike trains. In particular, we show that a presynaptic subgroup with an oscillatory firing rate embedded in a set of uncorrelated afferents can be biased towards potentiation or depression, depending upon the intrinsic dynamics of the postsynaptic neuron and the period of the modulation.

KEY WORDS
STDP · single neuron dynamics · intrinsic oscillations · network oscillations · learning · self-organization

1 Introduction

Experimental results have revealed a form of Hebbian learning which is extremely sensitive to the precise timing of pre and postsynaptic firing patterns. In particular, in paired-pulse experiments (where brief suprathreshold current pulses are injected in the pre and postsynaptic cell at a fixed temporal delay) LTP was observed when the evoked presynaptic spike led the postsynaptic spike (thus contributing to the postsynaptic cell firing), while LTD was observed when the evoked presynaptic spike lagged behind the postsynaptic one ([1, 2]; reviewed in [3, 4]).

In the last few years, several theoretical works have stemmed from this experimental observations, predicting an important role for STDP in self-organization of neural microcircuits [5, 6, 7, 8, 9], learning of input correlations [10, 11, 12], and output firing rate normalization [10, 13, 14].

While the influence of different STDP rules upon the weight dynamics and the stationary weight distribution has been studied extensively (reviewed in [15, 16]), only very recently there has been some attention drawn upon the influence of single-cell intrinsic properties in STDP dynamics [9]. The intrinsic dynamics of the postsynaptic cell determine the integration of subthreshold stimuli and the spike generation mechanism (see, for example, [17, 18, 19, 20]), thus directly affect the cross-correlation between the input and the output spike trains. This consideration suggests that the intrinsic postsynaptic dynamics can potentially have a great impact upon the weight dynamics arising from a certain STDP rule.

In this paper we consider a feedforward neuronal architecture where one postsynaptic cell receives a synaptic bombardment from several hundred presynaptic afferents, and compare the stationary weight distributions arising from the same STDP rule and presynaptic firing statistics, but different postsynaptic intrinsic properties. In particular, we compare a purely passive Integrate and Fire (IF) model with an inductive Generalized Integrate and Fire (GIF) model with subthreshold oscillations.

Our results suggest that the intrinsic properties of the postsynaptic cell quantitatively affect the stationary weight distribution under different STDP rules when the input firing patterns are uncorrelated. More interestingly, a sinusoidal modulation of the firing statistics of a subset of the presynaptic population reveal qualitative and important differences in the weight dynamics between the IF and the GIF model, which are the focus of this work.

2 Methods

2.1 Neuron models

The first neuron model we consider is the Integrate and Fire (IF), described by a single linear differential equation:

$$\frac{dv}{dt} = -gv + I_{syn} \tag{1}$$

The model is endowed with an after-spike reset mechanism, so that when v crosses a threshold v_{thr} from below a spike is emitted and the membrane potential is reset to a value v_{reset}, and kept there for a refractory period t_{refr}. In its normal form (where time has been properly scaled) this model is described by a single parameter g, which is the rate of the exponential decay to the rest state in the absence of stimulation ($I_{syn} = 0$).

Another simple model which linearly describes the subthreshold dynamics, with the addition of another dynamical variable w, is the Generalized Integrate and Fire (GIF) model, described by the following equations:

$$\begin{array}{rcl} \frac{dv}{dt} & = & -\alpha v - \beta w + I_{syn} \\ \frac{dw}{dt} & = & v - w \end{array} \quad (2)$$

with the same after-spike resetting as in the IF model for the v variable, while no reset is applied to the additional dynamical variable w. The system (2) has proven particularly useful in studying neuronal intrinsic oscillations [17, 21, 22, 18]: in a certain parameter range, the system (2) is mathematically equivalent to a dampened linear oscillator, and thus constitutes an analytically amenable model for the description of neuronal intrinsic oscillations, i.e., oscillations generated by intrinsic ionic mechanism as the activation of a resonant current or the inactivation of an amplifying current [23].

The numerical values of the parameters used here are: $v_{thr} = 20$, $v_{reset} = -4$, $t_{refr} = 0.3$, $g = 1$, $\alpha = 1$ and $\beta = 4$ (resulting in complex conjugate eigenvalues $-1 \pm 2i$, denoting subthreshold dampened oscillations with period π). All units are dimensionless.

2.2 Synaptic description

For the sake of simplicity, and for computational efficiency, we modelled PSPs as instantaneous, voltage independent shifts in the voltage variable:

$$I_{syn} = \sum_{n=1}^{N} \sum_{t_n^s} g_n^{syn} \delta(t - t_n^s) \quad (3)$$

where $N = 250$ is the number of afferents, and g_n^{syn} is the synaptic strength of afferent number n. We discretized the simulations in time steps of size $dt = 0.01$ u.t., and in each time step we generated a presynaptic input pattern in which each afferent which is not in its refractory period has a probability p_n of firing. Once an afferent has been selected for firing, it will not be able to generate another spike for $t_{refr} = 0.3$ u.t..

We divided the afferent population in three subsets: $N_{exc} = 170$ Poisson excitatory afferents with a constant firing probability $r_{exc} = 0.0033$, corresponding to a mean ISI of 3 u.t.; $N_{osc} = 30$ Poisson excitatory afferents with a sinusoidally modulated firing probability $r_{osc} = r_{exc} + A_{sin} r_{exc} \sin(\frac{2\pi}{T} t)$ with period $T = \pi$ (except in Figure 3 and 5 where it has been varied in a range, and in Figure 4 where $T = 1.2743$ or $T = 7.8476$) and modulation amplitude $A_{sin} = 0.5$; $N_{inh} = 50$ Poisson inhibitory afferents with a constant firing probability $r_{inh} = r_{exc} = 0.0033$. The synaptic strengths of the excitatory connections $g_n^{syn} = g_{syn}^{exc} w_n$ are obtained by multiplying the corresponding synaptic weights w_n (which are bounded in the interval [0,1] and subject to STDP) by a scaling factor $g_{syn}^{exc} = 4$. The synaptic strengths of the inhibitory connections are fixed at $g_{syn}^{inh} = 6$.

At the beginning of each simulation the synaptic weights w_n of the excitatory population are homogeneously initialized at their maximal value of 1. These values result in fast and regular postsynaptic firing at a frequency close to the maximal frequency allowed by the refractory period. In this regime the STDP weight dynamics strongly depress most synapses in a non-specific way (Figure 1A, B), until the postsynaptic neuron sets in a lower frequency irregular firing regime. The regular and the irregular firing regimes display large differences not only in their firing statistics, but also in their response to a sinusoidal modulation [17]. Thus we disregarded the first $30 \cdot 10^3$ u.t of the simulations output and focused our analysis on the subsequent evolution of the synaptic weights through STDP in the low frequency, irregular firing regime, during which the mean and the standard deviation of the output ISIs (Inter Spike Intervals) can be considered stationary, as well as the phase of the response to the sinusoidal modulation.

All the simulations have been run for $5 \cdot 10^6$ u.t. Convergence has been assured by visual inspection of the output data and it has always been reached within $2 \cdot 10^6$ u.t. of simulation time.

The sinusoidal modulation in the input rate induces a sinusoidal modulation of the firing probability, which we fit to a sinusoidal function $p_{offset} + A_g \sin(\frac{2\pi}{T} t + \phi)$ to obtain the modulation gain A_g and phase ϕ plotted in Figure 3, 4 and 5.

2.3 STDP model

The excitatory synaptic connections are plastic and evolve according to the STDP rule described in [11]. In brief, every pair of a presynaptic and a postsynaptic action potentials with time difference $\Delta t = t_{post} - t_{pre}$ induce a weight change given by

$$\Delta w = G(\Delta t|w) = \begin{cases} -\lambda f_-(w) K(\Delta t) & \text{if } \Delta t \leq 0 \\ \lambda f_+(w) K(\Delta t) & \text{if } \Delta t > 0 \end{cases} \quad (4)$$

where $K(\Delta t) = e^{-|\Delta t|/\tau}$ is the STDP window function, λ is a learning rate, and $f_\pm(w)$ describe the weight dependence of the STDP rule:

$$f_+ = (1-w)^\mu \qquad f_- = \alpha w^\mu \quad (5)$$

where α describes the asymmetry between depression and potentiation, and μ is a parameter included in [0,1] which determines the weight dependence of the STDP rule. If $\mu = 0$, $G(\Delta t|w)$ results is the familiar weight independent (additive) STDP rule like in [10]; if $\mu = 1$ one recovers the multiplicative STDP rule like in [14]. The numerical values for the parameters are: $\lambda = 0.002$, $\tau = 0.8$, $\alpha = 1.05$ and $\mu = 0.02$.

3 Results

Over time scales shorter than $1/\lambda$, the input-output correlation can be considered stationary and the mean weight

drift can be obtained from (4) by integrating over the time difference Δt, weighted by its correspondent probability:

$$\dot{w} = \int_{-\infty}^{\infty} G(\Delta t|w) P_t(\Delta t|w) d\Delta t \qquad (6)$$

The dependence upon the intrinsic neuronal properties of the postsynaptic cell is included in the input-output correlation term $P_t(\Delta t|w) =< \rho^{pre}(t)\rho^{post}(t+\Delta t, w) >_t$ where $\rho^{pre}(t) = \sum_k \delta(t-t_k^{pre})$ and $\rho^{post}(t,w) = \sum_k \delta(t-t_k^{post})$ are the pre and postsynaptic spike trains, and $< \cdot >_t$ indicates averaging over time.

The postsynaptic intrinsic properties affect the integration of incoming stimuli, and determine the input-output transformation performed. For instance, an EPSP evoked on a regular spiking neuron at a certain point of its firing cycle can have an excitatory or an inhibitory effect depending upon the intrinsic properties of the postsynaptic neuron [20, 24, 25, 26].

Intrinsic neuronal properties (in particular, intrinsic oscillations) affect the neuron's behavior in response to a sinusoidal modulation [17]. While a purely passive neuron like an IF always follows the sinusoidal modulation with some delay, a GIF neuron with intrinsic oscillations can synchronize to an input modulation or even lead ahead of it, depending upon the intrinsic resonant frequency and the frequency of the sinusoidal modulation ([17], see also Figure 3A).

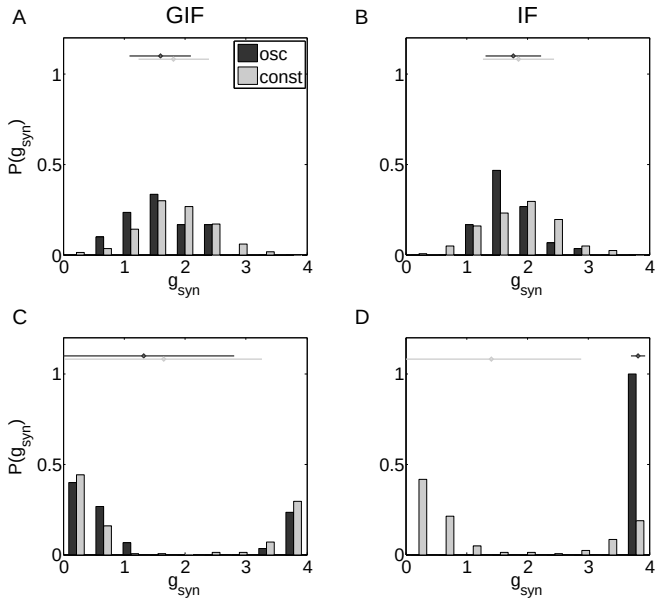

Figure 1. Intrinsic neuronal properties determine the dynamics and the equilibrium distribution of the weights under STDP. Distributions of the synaptic weights for the GIF (left) and IF (right) neuron model at the beginning of the low frequency, irregular firing regime (top) and at equilibrium (bottom). For each afferent population, the diamond indicates the mean of the weight distribution and the horizontal line its standard deviation. In the initial high frequency, regular firing regime the synapses are depressed in a non-specific way and reach a unimodal distribution where the oscillatory and non-oscillatory populations overlap (A, B). After learning, the weight distributions are bimodal for both neuron types but while the two populations are still largely overlapping for the GIF neuron (C), the oscillatory population is significantly more potentiated for the IF neuron (D).

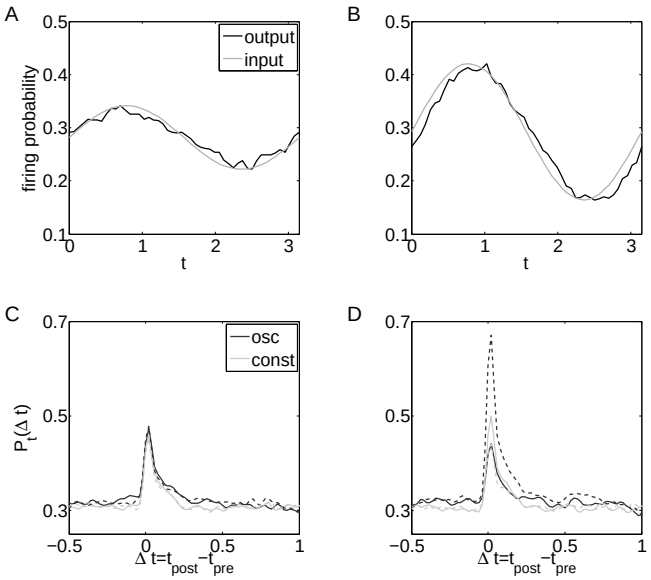

Figure 2. Intrinsic neuronal properties determine the phase of the oscillating response, and hence the input-output cross-correlation. A, B: The firing probability along the cycle at the end of the simulation (black line) is plotted together with the sinusoidal modulation of the input firing rate (gray). While the output is in phase with the input for the GIF neuron, there is a delay for the IF neuron. Moreover, the gain in the IF neuron is increased due to potentiation of the oscillating population. C, D: $P_t(\Delta t)$ is plotted for the oscillatory (black) and non-oscillatory (gray) population for the GIF (solid line) and IF (dashed line) neuron at the beginning of the irregular firing regime (left) and at the end of the simulation (right). At the beginning of the irregular firing regime the oscillating afferents are slightly more efficient in firing the postsynaptic cell due to their common sinusoidal modulation. This can be deduced from the broader input-output correlation and the higher peak, but little difference can be observed between cell types, apart from a slight excess of negative (depressing) Δt pairs in the GIF neuron. After learning the input-output correlation has clearly increased for the oscillating subgroup in the IF neuron, which also exhibits an excess of positive (potentiating) Δt pairs.

When the synaptic afferents to a neuron are composed of two different populations, one with a constant firing frequency and another with a sinusoidally modulated firing frequency, the phase with which the postsynaptic neuron follows the sinusoidal modulation determines if the oscillating population will differentiate from the non-oscillating population, and in which direction, through the STDP dynamics. Indeed, an IF neuron which follows a sinusoidal modulation with a phase delay will on average fire after most of the neurons in the oscillating population (Figure 2B), leading to a selective strengthening of the synapses

belonging to this group (Figure 1D). Conversely, the GIF neuron follows the same sinusoidal modulation without any significant phase difference (Figure 2A), hence its spikes will be symmetrically distributed with respect to the oscillating population (Figure 2C, D), leading to no net potentiation nor depression with respect to the non-oscillating population (Figure 1C).

To quantify the degree of separation between the oscillating and the non-oscillating populations, we computed the ratio between the mean conductance in the two subgroups $R =< g_{osc} > / < g_{const} >$. Figure 3 shows the relationship between R and the phase of the sinusoidal response: as expected from our theoretical considerations, the sign of the phase lag determines if the oscillating subgroup will be potentiated or depressed. A negative phase (the postsynaptic neuron lags behind the sinusoidal modulation) results in relative potentiation of the oscillating subgroup of afferents ($R > 1$), while a positive phase leads to relative depression of the oscillatory population ($R < 1$). This general relationship does not hold for very short input periods T, for which a very negative phase results in no differentiation or only slight potentiation of the oscillating subgroup: at very high input frequencies a postsynaptic spike lagging behind a given cycle can also be considered as leading ahead the next cycle, so that as soon as the STDP window becomes comparable in width with the input oscillation period the effects of potentiation and depression tend to cancel out. Measures of the separation between the two different populations which also take into account the standard deviation of the two distributions yielded similar results. In spite of this general tendency, there are some additional differences between the GIF and the IF models which cannot be explained solely on the basis of the phase of the sinusoidal response. For example, for a certain range of negative phase lags there is a stronger potentiation of the oscillating subgroup in the GIF neuron.

The cell-specific potentiation or depression of the oscillating population affects in turn the postsynaptic firing statistics, and in particular the gain of the oscillatory component of the postsynaptic response (Figure 4 and 5). In particular, a sinusoidal modulation which results in negative phase lag (the postsynaptic cell lags behind the sinusoidal modulation) leads to a selective strengthening of the oscillatory population, which in turn produces an increase in the sinusoidal gain. The opposite trend is observed for modulation periods and postsynaptic intrinsic properties which result in positive phase lag (the postsynaptic cell leads ahead of the sinusoidal modulation). This dynamics is shown in Figure 4, where the amplitude gain A_g and the separation index R are plotted for the GIF and IF neurons along a typical simulation for two representative values of the modulation period T. For short modulation periods ($T = 1.2743$ in the plotted example, the non-integer values are due to the logarithmically spaced values for T) both GIF and IF neurons lag behind the sinusoidal modulation, their oscillating afferents are potentiated and their sinusoidal gain is consequently increased. For modulation

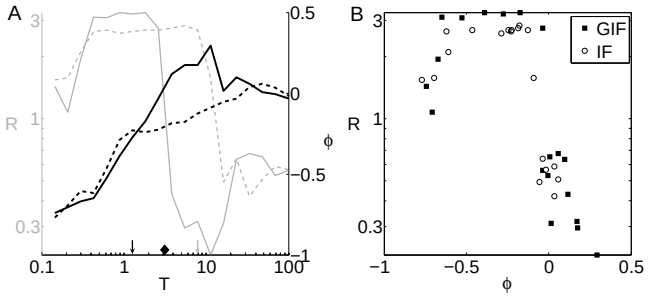

Figure 3. The phase of the sinusoidal response determines the mean drift of the oscillating population. A: Ratio between the mean oscillatory conductance and the mean non-oscillatory conductance $R =< g_{osc} > / < g_{const} >$ and phase of the sinusoidal response ϕ for the GIF (solid line) and IF (dashed line) models as a function of the period of the sinusoidal modulation. While the IF neuron always lags behind, the GIF neuron can synchronize with or even lead ahead of the sinusoidal input modulation. The sign of the phase determines the potentiation ($R > 1$) or depression ($R < 1$) of the oscillating population with respect to the other afferents. The black diamond indicates the intrinsic period for the GIF neuron considered, and the input period used in the simulations plotted in Figure 1. The black and the gray arrows indicate the input periods used in the simulations plotted in Figure 4. B: R ratio for the GIF (filled squares) and IF (empty circles) models after learning is plotted versus the correspondent phase.

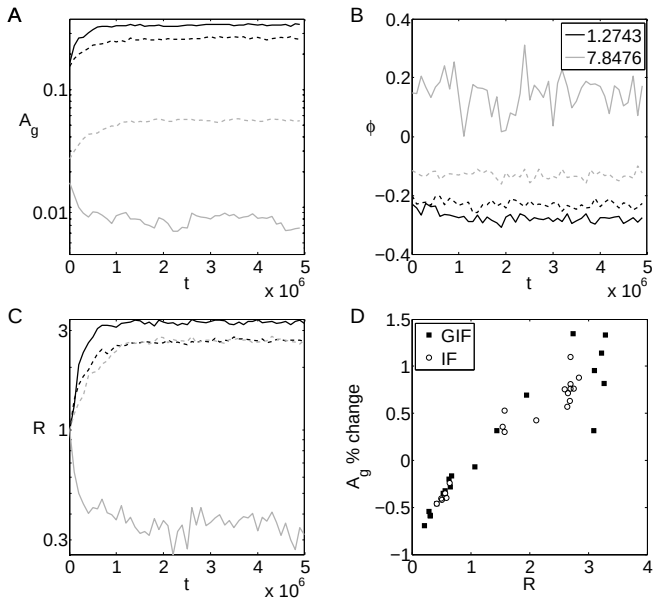

Figure 4. Evolution of some relevant quantities along a typical simulation for the GIF (solid line) and IF (dashed line) model, for two different values of the input modulation period. A: Sinusoidal gain A_g. B: Sinusoidal phase ϕ. C: R ratio. D: The relative potentiation of the oscillating population is the main determinant of the change in the sinusoidal gain due to STDP.

periods slightly greater than the intrinsic period π, the GIF and the IF neurons behave in a qualitative different way:

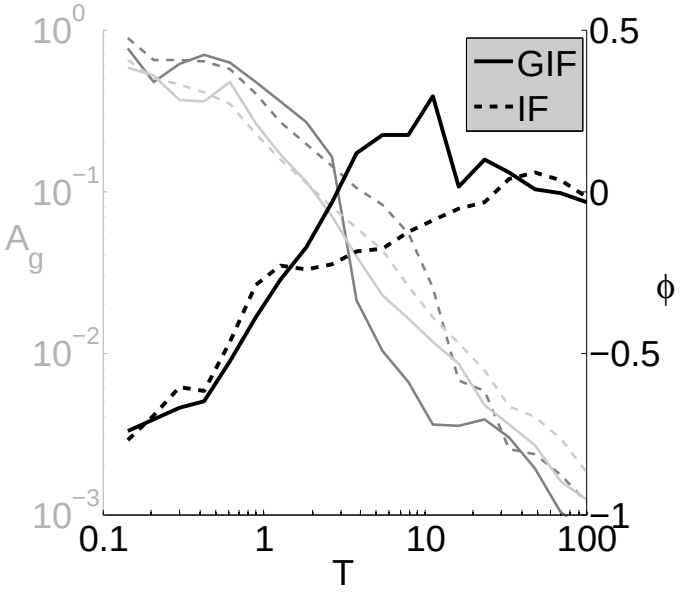

Figure 5. Gain and phase of the sinusoidal modulation as a function of the period T of the modulation. The gain is plotted at the beginning of the irregular firing regime (light gray) and at the end of the simulation (dark gray).

the IF neuron still lags behind the sinusoidal modulation, while the GIF neuron leads ahead of it, resulting in an opposite trend in their separation index R and consequently in their gain A_g (compare panels A and C). This cell-specific regulation of the sinusoidal gain through STDP is also apparent in Figure 5, where the gain for the GIF (solid) and IF models (dashed) is plotted at the beginning (light gray) and at the end (dark gray) of the simulations, for input periods T spanning three orders of magnitude. For all tested input periods, the difference in gain is very small at the beginning of the simulation, but it increases dramatically through the action of STDP for those input periods which result in qualitatively different behavior in the GIF and IF neuron (with T in the interval $(4, 20)$ approximately, the phase is positive for the GIF neuron and negative for the IF neuron). Conversely, the difference in gain between the two neuron models are negligible for very short or very long modulation periods, for which the two models display similar phase shifts.

To further clarify the relation between the R index and the sinusoidal gain, we lumped all the data obtained with different T for the same neuron model, and plotted the percentual change in sinusoidal gain A_g during learning versus R for the GIF (filled squares) and IF models (empty circles) (Figure 4D). This figure shows that the relationship between the sinusoidal gain change and the oscillating / non-oscillating ratio R is almost linear, with a R value of 1 (indifferentiation between the two subgroup of afferents) resulting in no gain change, suggesting that the changes in the sinusoidal gain observed during a simulation are mainly due to the relative potentiation or depression of the oscillating subgroup.

In our implementation, the sinusoidal gain increases with increasing input frequency, contrary to intuition and the results of others [17]. This discrepancy is probably due to the different implementation of the oscillatory component: while Richardson *et. al.* used a sinusoidal input current, we considered a sinusoidal modulation in the firing rate of a subgroup of afferents. Since in our model synapses are instantaneous (they are implemented as an instantaneous, voltage independent shift in the v variable), the sinusoidal modulation bypasses the low-pass filtering properties of the neuron models, resulting in unrealistically high gain at high input frequencies. Nevertheless, we believe that the described effect of STDP on the sinusoidal gain is general and probably applies to more realistic models as well.

The effect of STDP on the phase lag of the different model neurons is somewhat subtler. When the postsynaptic neuron lags behind the sinusoidal modulation, the oscillating afferents are potentiated with respect to the other afferents, and keep the postsynaptic cell at a constant, negative phase. Conversely, when the postsynaptic neuron leads ahead of the sinusoidal modulation, the oscillating afferents are depressed and their entrainment of the postsynaptic cell is less efficient, resulting in low sinusoidal gain and variable, positive phase (Figure 4C).

4 Conclusions

Intrinsic neuronal properties may affect the integration of incoming stimuli in a nontrivial way. For instance, an EPSP evoked on a regular spiking neuron can advance or delay the occurrence of the next spike, depending upon the intrinsic properties of the postsynaptic neuron and the exact time in which it is delivered.

Intrinsic neuronal properties (in particular, intrinsic oscillations) affect the neuron's behavior in response to a sinusoidal modulation embedded in a random synaptic bombardment [17]. While a purely passive neuron like an IF always follows the sinusoidal modulation with some delay, a GIF neuron with intrinsic oscillations can synchronize to an input modulation or even lead ahead of it, depending upon the intrinsic resonant frequency and the frequency of the sinusoidal modulation.

The phase of the sinusoidal response determines the net drift that will affect the weights of the oscillating population: if the phase is positive (the postsynaptic neuron leads ahead of the presynaptic sinusoidal modulation) the oscillating population will experience a net depressing effect (most postsynaptic spikes will lead the presynaptic spikes originating from this population), while if the phase is negative (the postsynaptic neuron follows the sinusoidal modulation with some delay) the oscillating population will be potentiated.

In our model, the oscillating population follows a sinusoidally modulated Poisson statistics, without any additional temporal structure. Hence, if the postsynaptic cell is

in phase with the input modulation, one particular presynaptic neuron will sometimes lead, sometimes lag the postsynaptic response so that the mean synaptic drift it will experience is zero. Conversely, if additional temporal structure were imposed on the oscillating population, a differentiation of the oscillating population from the rest of the afferents could still be observed. For instance, if a subset of the oscillating population were imposed to fire earlier on average than the other afferents of the oscillating population, this subset would be expected to undergo potentiation.

The net weight drift experienced by the oscillating population affects in turn the postsynaptic firing statistics. If the postsynaptic neuron follows the sinusoidal modulation with some delay, as in the case of the passive IF neuron, the oscillating population will undergo potentiation and will increase the gain of the sinusoidal modulation. Conversely, if the postsynaptic neuron is synchronized with the sinusoidal modulation, the net weight drift on the oscillating population will be the same as the one experienced by the other afferents, hence the sinusoidal gain will stay constant.

Thus, it seems that STDP might have a regulatory effect upon the sinusoidal gain in the presence of oscillatory inputs, by increasing the oscillatory input to target cells which follow the modulation with some delay, while not affecting or even decreasing the oscillatory inputs to target cells which display intrinsic oscillations in resonance with the frequency of the oscillatory modulation.

Since both network oscillations and intrinsic resonant neurons are widespread in many brain areas, we believe that this mechanism might be highly relevant for information processing and structure formation during both development and mature life, and might shed some light on the complex interplay between network oscillations and the heterogeneity of intrinsic neuronal dynamics.

Acknowledgements:
This work was supported by MEC BFU2006-07902/BFI and CAM S-SEM-0255-2006.

References

[1] H. Markram, J. Lübke, M. Frotscher, and B. Sakmann. Regulation of synaptic efficacy by coincidence of postsynaptic aps and epsps. *Science*, 275(5297), 1997, 213–215.

[2] G. Q. Bi and M. M. Poo. Synaptic modifications in cultured hippocampal neurons: dependence on spike timing, synaptic strength, and postsynaptic cell type. *J Neurosci*, 18(24), 1998, 10464–10472.

[3] Y. Dan and M. M. Poo. Spike timing-dependent plasticity of neural circuits. *Neuron*, 44(1), 2004, 23–30.

[4] G. Bi and M. Poo. Synaptic modification by correlated activity: Hebb's postulate revisited. *Annu Rev Neurosci*, 24, 2001, 139–166.

[5] E. V. Lubenov and A. G. Siapas. Decoupling through synchrony in neuronal circuits with propagation delays. *Neuron*, 58(1), 2008, 118–131.

[6] S. Kang, K. Kitano, and T. Fukai. Structure of spontaneous up and down transitions self-organizing in a cortical network model. *PLoS computational biology*, 4(3), 2008.

[7] R. Kempter, C. Leibold, H. Wagner, and J. L. van Hemmen. Formation of temporal-feature maps by axonal propagation of synaptic learning. *Proc Natl Acad Sci U S A*, 98(7), 2001, 4166–4171.

[8] S. Song and L. F. Abbott. Cortical development and remapping through spike timing-dependent plasticity. *Neuron*, 32(2), 2001, 339–350.

[9] H. Câteau, K. Kitano, and T. Fukai. Interplay between a phase response curve and spike-timing-dependent plasticity leading to wireless clustering. *Physical review. E, Statistical, nonlinear, and soft matter physics*, 77(5 Pt 1), 2008, 051909.

[10] S. Song, K. D. Miller, and L. F. Abbott. Competitive hebbian learning through spike-timing-dependent synaptic plasticity. *Nat Neurosci*, 3(9), 2000, 919–926.

[11] R. Gütig, R. Aharonov, S. Rotter, and H. Sompolinsky. Learning input correlations through nonlinear temporally asymmetric hebbian plasticity. *J Neurosci*, 23(9), 2003, 3697–3714.

[12] H. Meffin, J. Besson, A. N. Burkitt, and D. B. Grayden. Learning the structure of correlated synaptic subgroups using stable and competitive spike-timing-dependent plasticity. *Physical review. E, Statistical, nonlinear, and soft matter physics*, 73(4 Pt 1), 2006, 041911.

[13] J. Tegnér and A. Kepecs. An adaptive spike-timing-dependent plasticity rule. *Neurocomputing*, 44-46, 2002, 189–194.

[14] J. Rubin, D. D. Lee, and H. Sompolinsky. Equilibrium properties of temporally asymmetric hebbian plasticity. *Physical Review Letters*, 86(2), 2001, 364–367.

[15] A. Morrison, M. Diesmann, and W. Gerstner. Phenomenological models of synaptic plasticity based on spike timing. *Biological Cybernetics*, 98(6), 2008, 459–478.

[16] A. Kepecs, M. C. van Rossum, S. Song, and J. Tegner. Spike-timing-dependent plasticity: common themes and divergent vistas. *Biological Cybernetics*, 87(5-6), 2002, 446–458.

[17] M. J. Richardson, N. Brunel, and V. Hakim. From subthreshold to firing-rate resonance. *J Neurophysiol*, 89(5), 2003, 2538–2554.

[18] S. Schreiber, I. Erchova, U. Heinemann, and A. V. Herz. Subthreshold resonance explains the frequency-dependent integration of periodic as well as random stimuli in the entorhinal cortex. *J Neurophysiol*, 92(1), 2004, 408–415.

[19] F. Baroni and P. Varona. Subthreshold oscillations and neuronal input-output relationships. *Neurocomputing*, 70(10-12), 2007, 1611–1614.

[20] B. S. Gutkin, B. G. Ermentrout, and A. D. Reyes. Phase-response curves give the responses of neurons to transient inputs. *J Neurophysiol*, 94(2), 2005, 1623–1635.

[21] T. Verechtchaguina, I. M. Sokolov, and L. Schimansky-Geier. Interspike interval densities of resonate and fire neurons. *Biosystems*, 89(1-3), 2007, 63–68.

[22] E. M. Izhikevich. Resonate-and-fire neurons. *Neural Netw*, 14(6-7), 2001, 883–894.

[23] B. Hutcheon and Y. Yarom. Resonance, oscillation and the intrinsic frequency preferences of neurons. *Trends Neurosci*, 23, 2000, 216–222.

[24] R. F. Galan, B. G. Ermentrout, and N. N. Urban. Efficient estimation of phase-resetting curves in real neurons and its significance for neural-network modeling. *Physical Review Letters*, 94(15), 2005, 158101.

[25] S. A. Oprisan and C. C. Canavier. The influence of limit cycle topology on the phase resetting curve. *Neural computation*, 14(5), 2002, 1027–1057.

[26] B. Ermentrout. Type i membranes, phase resetting curves, and synchrony. *Neural computation*, 8(5), 1996, 979–1001.